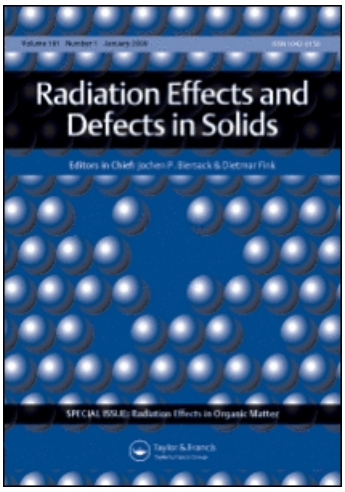

Radiation Effects and Defects in Solids
Publication details, including instructions for authors and subscription information:
http://www.informaworld.com/smpp/title~content=t713648881

On the redistribution of 10keV hydrogen in $CuInSe_2$

D. Fink [a]; J. Krauser [a]; G. Lippold [b]; M. V. Yakushev [c]; R. D. Tomlinson [c]; A. Weidinger [a]; K. K. Dwivedi [ad]; S. Ghosh [ac]; W. H. Chung [ef]
[a] Hahn-Meitner-Institut, Berlin, Germany [b] Fakultät für Physik und Geowissenschaften, Universität Leipzig, Leipzig, Germany [c] Department of Physics, University of Salford, Salford, UK [d] Department of Chemistry, North-Eastern Hill University, Shillong, India [e] Department of Chemistry, Sankardov College, Shillong, India [f] Department of Physics, Pusan National University, Pusan, Korea

Online Publication Date: 01 July 1998

To cite this Article Fink, D., Krauser, J., Lippold, G., Yakushev, M. V., Tomlinson, R. D., Weidinger, A., Dwivedi, K. K., Ghosh, S. and Chung, W. H.(1998)'On the redistribution of 10keV hydrogen in $CuInSe_2$',Radiation Effects and Defects in Solids,145:1,85 — 105
To link to this Article: DOI: 10.1080/10420159808220025
URL: http://dx.doi.org/10.1080/10420159808220025

Radiation Effects & Defects in Solids, Vol. 145, pp. 85–105
Reprints available directly from the publisher
Photocopying permitted by license only

ON THE REDISTRIBUTION OF 10 keV HYDROGEN IN $CuInSe_2$

D. FINK [a,*], J. KRAUSER [a], G. LIPPOLD [b], M.V. YAKUSHEV [c], R.D. TOMLINSON [c], A. WEIDINGER [a], K.K. DWIVEDI [a,d], S. GHOSH [a,e] and W.H. CHUNG [a,f]

[a] *Hahn-Meitner-Institut, Glienicker Str. 100, D-14109 Berlin, Germany;* [b] *Fakultät für Physik und Geowissenschaften, Universität Leipzig, Linnestr. 5, D-04103 Leipzig, Germany;* [c] *Department of Physics, University of Salford, Salford M5 4WT, UK;* [d] *Department of Chemistry, North-Eastern Hill University, Shillong-793 003, India;* [e] *Department of Chemistry, Sankardov College, Shillong-793 003, India;* [f] *Department of Physics, Pusan National University, Pusan 609-735, Korea*

(Received 12 September 1997; Revised 20 October 1997; In final form 24 November 1997)

20 keV H_2^+, corresponding to 10 keV H, was implanted at room temperature into Bridgman-grown single crystalline $CuInSe_2$ at doses of 1×10^{15}, 1×10^{16}, and 1×10^{17} H/cm^2. Using the ^{15}N nuclear reaction method, the hydrogen depth profile was studied in order to investigate the hydrogen diffusion mechanism and to estimate a diffusion coefficient. The hydrogen depth distribution in the as-implanted samples revealed considerable deviations from the expected ballistic range profiles. The H redistribution was simulated by a numerical computer calculation. The best fit between measurements and simulations was obtained by assuming that

(a) this material does not contain intrinsic *deep* traps for the mobile hydrogen implants,
(b) this material contains a broad distribution of intrinsic *shallow* and additionally irradiation-induced surface-near traps,
(c) the detrapping efficiency from these traps decreases with increasing dose, and
(d) the depth distribution of these shallow traps ranges from the surface down to about 400 nm depth, i.e. beyond the hydrogen range.

Subsequent thermal annealing up to 200°C for half an hour led to minor changes of the hydrogen profiles at the highest implantation dose, and to major changes at the intermediate dose of 10^{16} cm^{-2}. All the changes of the hydrogen depth distributions can be described by the same set of assumptions, though their numerical values differ somewhat from the as-implanted case, due to additional thermal hydrogen mobility.

* Corresponding author.

Keywords: Hydrogen; $CuInSe_2$; Ion implantation; High dose; Diffusion; Trapping; Detrapping; Unsaturable traps; ^{15}N nuclear reaction analysis; Simulations; Finite difference technique

1. INTRODUCTION

The ternary chalcopyrite semiconductor $CuInSe_2$ is a promising material for polycrystalline thin film solar cell applications. In a few recent studies, properties of hydrogen-implanted $CuInSe_2$ have been investigated. In [1,2] for example, the defect production as a result of the hydrogen implantation has been studied. Whereas high doses above about $N = 1 \times 10^{16}\,H/cm^2$ were found to induce lattice damage which saturates at doses above $N = 1 \times 10^{17}\,H/cm^2$, low doses below about $N = 2 \times 10^{15}\,H/cm^2$ improve the lattice quality as compared with the virgin crystal. This was explained by an atomic hydrogen related defect passivation effect. Defect passivation due to the formation of hydrogen–defect bonds was also assumed to be responsible for changes in photoluminescence and improved photoresponse of hydrogen implanted solar cell structures [3]. Hydrogen implantation into p-type $CuInSe_2$ was found to produce an n-type implanted layer and, therefore, a p–n homojunction, the thermal stability of which is limited to temperatures below 100°C [4]. In all of these works, the assumption of a high mobility of atomic hydrogen in $CuInSe_2$ even at room temperature was necessary to explain the experimental findings [5].

The aim of this work is to investigate the redistribution of ion-implanted hydrogen in single crystalline $CuInSe_2$ during subsequent annealing, in order to study the diffusion mechanism, to measure diffusion coefficients and to correlate them with various defect concentrations resulting from different implanted doses.

It has often been observed that, after implantation of light ions such as H, He, Li, B, N, and F into solids at room temperature, the implanted ions do not distribute strictly according to their theoretically predicted ballistic implantation profiles, but that sometimes their distributions are found to be broadened by diffusion. In other cases, the ions' nuclear and/or electronic energy transfer dominates their redistribution. Here, the behavior of the implanted ions strongly depends on the projectile's energy dose, and atomic number and on the target

atomic number and density, hence on both the projectile's stopping power and the deposited energy density in the target. Whereas irradiation with light projectiles at low doses allows one to study the action of simple defects such as interstitials and vacancies onto the dopant mobility, the use of heavier ions, or of light ions at elevated doses complicates the picture considerably. Here the additional effect of more complex defect structures – such as interstitial or vacancy clusters, dislocations and/or precipitations – can no longer be neglected. In order to understand the transition from the action of simple defects onto the dopant distribution towards the effect of more complex ones, we have performed first systematic experiments by implanting hydrogen ions into $CuInSe_2$ at increasing doses, but at else identical conditions.

The analysis of the diffusionally broadened hydrogen depth profiles should, therefore, give us essentially information about the intrinsic and ion-induced defect population in the examined material, as defects act as saturable or unsaturable trapping centers. *Saturable traps* are capable to bind only a well-defined number of probe atoms (typically one to six), whereas *unsaturable traps* can bind in the ideal case an unlimited amount of dopants, thus acting as nucleation centers for bubbles or precipitates.

Further one has to distinguish between shallow and deep traps. *Shallow traps* (i.e. traps with low bonding energy to probe atoms) release the bound dopant atoms again after some time, whereas *deep traps* will rather bind the dopant atoms permanently. Hence, for shallow traps: $0 < A < 1$ and $0 < B < 1$, the trap strength being the lower the more A approaches B. For deep traps: $A \gg 0$, $A \leq 1$, and $B \approx 0$, so that $B/A \approx 0$, with A and B being the probabilities for trapping and detrapping from these traps, respectively. In other words, the existence of shallow traps in a sample lowers the overall diffusional coefficient of the probe atoms from the one in an ideal defect-free material, D_0, towards an "effective" diffusion coefficient $D_{\text{eff}} \approx D_0/(1 + A/B)$, the so-called diffusion coefficient of "hindered" or "trapping–detrapping" mobility. For contrast, the presence of deep traps totally prevents the dopant mobility at the trap location at all.

The concept to describe the counterplay of mobile and trapped impurities in the presence of saturable and unsaturable traps by means of rate equations has been successfully applied to semiconductors for a long time [6]. That theory is restricted to the *overall* mobile and trapped

dopant populations at both saturable and unsaturable traps in a given sample, without taking into account their depth dependence. The latter drawback has been overcome by us recently by writing a numerical computer code for simulation of depth dependent diffusion in the presence of depth dependent saturable and unsaturable trap distributions. With this code deviations of hydrogen implantation profiles in silicon from predicted distributions after low dose implantation could already be treated successfully [7]. Furthermore, we have recently used this code to treat the radiation enhanced diffusion of ion-implanted Li in polypropylene foils [8], and the soaking of ion-irradiated polyethyletherketone (PEEK) foils with aqueous LiCl solution [9]. In this work we describe the first application of this code to the semiconductor material $CuInSe_2$.

2. SAMPLE PREPARATION AND MEASUREMENT

For the experiments we used vertical Bridgman-grown single crystalline $CuInSe_2$. The sample was cut from the middle part of an ingot using a wire saw. In an EDX measurement, the composition of the p-type material was found to be Cu: 25.7 at%, In: 24.6 at%, Se: 49.7 at%. Taking into account the uncertainties in this determination, the sample may be considered as stoichiometric or slightly Cu-rich. In the latter case some Cu_xSe precipitates may be present and influence the measured hydrogen diffusion. However, one should bear in mind that other defects in the sample, if finely dispersed, may influence the hydrogen diffusion more strongly, even if their concentration is low. In any case, the measured hydrogen diffusion coefficients must be considered as the effective ones for the specific sample under consideration.

In our study, the diffusion of the implanted hydrogen is sensitive to a defect profile in a near-surface range of the sample. Therefore, special care must be taken in the surface preparation prior to the hydrogen implantation in order to avoid an additional defect background. As shown in [10], even careful polishing introduces defect profiles as deep as 30 nm into the $CuInSe_2$ crystal, which can be removed by annealing. Prior to the hydrogen implantation, the sample was polished with 3 μm and 1 μm diamond paste and finally with 0.05 μm Al_2O_3 powder in a vibrator bath. In order to remove the polish-induced defects without a

change in surface composition, the sample was annealed in vacuum together with $CuInSe_2$ powder at 400°C for 2 h. The implantation was performed at room temperature using an ion implanter, equipped with a magnetic mass separator. With a beam current density of 5 μA/cm^2, H_2^+ ions were implanted at doses of $N = 1 \times 10^{15}$ H/cm^2, 1×10^{16} H/cm^2 and 1×10^{17} H/cm^2 into about 4 mm broad stripes, leaving one area unimplanted as a reference. The ionized H_2^+ molecules were implanted with an energy of 20 keV, but can be expected to split into 10 keV atomic hydrogen when hitting the sample. As the vacuum during the implantation was only in the order of about 10^{-3} Pa, the $CuInSe_2$ surface was somewhat contaminated with residual hydrocarbons.

Prior to the hydrogen depth profiling, Raman measurements were performed to study the implantation-induced lattice damage. Because of the assumed high hydrogen mobility, care must be taken to avoid changes in the hydrogen distribution due to laser annealing during the Raman measurements. Therefore, we studied the implant damage using a micro-Raman technique. The excitation laser beam of a 514.5 nm Ar^+ ion laser with a power of 1 mW was focused to 1 μm in diameter. We cannot actually exclude an increased hydrogen diffusion during the Raman measurement, but it is limited to an area of a few μm^2 only. This is only about 10^{-6} of the area, sampled during the ^{15}N hydrogen depth profiling and, therefore, without significant influence on these measurements.

With the implanted doses, typical H concentrations from 3×10^{19} to 5×10^{21} ions/cm^3 (about 0.03–5% atomic) are obtained. The use of the $^1H(^{15}N, \alpha\gamma)^{12}C$ reaction is increasingly favored for hydrogen depth profiling since it was first introduced by Lanford *et al.* [11] in 1976. This is due to its excellent depth resolution and its good sensitivity. The experimental setup for this nuclear reaction analysis (NRA) at the Hahn-Meitner-Institut (HMI) Berlin is described elsewhere in detail [12]. During profiling, the samples were cooled to 80 K by liquid nitrogen to prevent hydrogen migration under the influence of the analyzing beam. Analyzing beam currents were typically between 200 and 300 nA. Here the integrated charge per data point was 30 μC (i.e. 200 nA, 150 s) in order to reach sufficient statistical accuracy. The measurements were performed in a vacuum better than 4×10^{-6} Pa, and the system is calibrated using a sample of amorphous silicon (a:Si–H) with known hydrogen concentration as a standard. The hydrogen depth profile

measurements took place about 3 weeks after the implantation. After recording the as-implanted hydrogen depth profiles, the samples were annealed at 473 K for 30 min at 10^{-5} Pa. Subsequently, the samples were cooled down to 80 K again and hydrogen depth profiling was repeated under the same experimental conditions as described above without ever leaving the vacuum chamber.

For the conversion of the ^{15}N beam energy loss to a hydrogen depth scale, a stopping power of $dE/dx = 2.15\,keV/nm$ was taken according to TRIM [13]. The absolute overall accuracy of the measurement is in the order of 10%.

3. THE COMPUTER CODE FOR DIFFUSIONAL SIMULATIONS OF DOPANTS IN SOLIDS WITH SATURABLE AND UNSATURABLE TRAPS

Let us assume that the H atoms under consideration here move in the target with a depth (x) dependent diffusion coefficient $D(x)$, until they are trapped in either depth dependent saturable or unsaturable traps, with probability rates for trapping being given by $A_s(x)$ and $A_u(x)$, respectively. Let us further define $B_s(x)$ and $B_u(x)$ as the depth dependent probability rates for detrapping from saturable and unsaturable traps, respectively. Then the differential equations which govern the overall dopant behavior are:

$$\frac{dC_f}{dt} = D\frac{\partial^2 C_f}{\partial x^2} - (A_s + A_u)C_f + B_s C_s + B_u C_u, \tag{1}$$

$$\frac{dC_s}{dt} = A_s C_f - B_s C_s, \tag{2}$$

$$\frac{dC_u}{dt} = A_u C_f - B_u C_u, \tag{3}$$

where $C_f = C_f(x, t)$, $C_s = C_s(x, t)$, and $C_u = C_u(x, t)$ denote the concentrations of free and trapped atoms in saturable and unsaturable traps, respectively. This system of differential equations is one dimensional only, i.e. it depends only on the depth as variable parameter, but it does not describe the atoms' lateral mobility. Therefore, it is strictly applicable only to homogeneous media, as given in our case.

A numerical computer program based on the 'finite difference method' has been written to solve the above introduced system of differential equations. In this approach the whole depth profile of a given distribution is divided into single channels. The program simulates any given diffusion problem by applying iteratively (i times) an elemental numerical diffusion step. The simulation is described by the relation:

$$Dt = iqW^2, \tag{4}$$

where D is the diffusion coefficient of the diffusing specie, t is the diffusion time, and W is the channel width of the numerical calculation. q is the fraction of diffusional redistribution per channel in an elemental simulation step. In general, q is chosen to be 1/3 for the simulation of diffusional problems with depth independent diffusion coefficients. For simulation of diffusional redistribution with depth dependent diffusion coefficients: $D(x) = D_{\max} \cdot f_D(x)$. The factor q is set to $q(x) = f_D(x)/3$, with $f_D(x) \leq 1$ describing the depth dependence of the diffusion coefficient. As the speed of diffusional broadening of depth profiles changes with i^{-2}, we plot every i^2th depth profile only. Thus one obtains equidistant curves in the case of regular (i.e. Fickian) diffusion.

As the initial concentration profile, we have taken the purely ballistic range profile prediction as given by Biersack's computer code TRIM [13]. This makes sense as long as the implant concentration is so small that sputtering, swelling and stoichiometric saturation effects still can be neglected. In our experiment this is definitely the case for the 10^{15} and $10^{16}\,cm^{-2}$ implantation. However, the maximum concentration after the $10^{17}\,cm^{-2}$ implantation being in the order of already a few percent atomic, one might expect in this case the onset of profile distortions. Nevertheless we applied also in this case for simplicity the purely ballistic TRIM code, as the measured deep hydrogen profiles (see below) indicate that diffusional effects dominate the ballistic ones by far.

It was mentioned in the introduction that the action of shallow traps is just to reduce the overall dopant mobility so that an effective diffusion coefficient could be defined, which depends only on the ratio A/B. This signifies a great simplification of the diffusion simulation task according to Eqs. (1–3). It also signifies, however, that in case of

shallow traps existing in a sample, only the ratio A/B can be determined, but not the absolute values of both B and A.

The diffusion coefficients derived by best-fit simulations of a given concentration profile are not necessarily the true diffusion coefficient values D_0 of the pure (i.e. defect-free) material. In presence of a homogeneous background of shallow traps, the derived diffusion coefficient rather has the meaning of an effective one. This is, in fact, the case for $CuInSe_2$ which is known to be not defect-free.

This approach is based on the assumption that both A and B are time independent, i.e. that self-annealing of the corresponding defects does not occur. If this were not the case, the applied program would have to be modified. As at present, there does not yet exist any hint for defect self-annealing in $CuInSe_2$, we used the code as described above.

4. RESULTS AND DISCUSSION

The Raman spectra are shown in Fig. 1. Whereas no radiation damage is found in the $N = 1 \times 10^{15}\,H/cm^2$ implantated area, the $N = 1 \times 10^{16}\,H/cm^2$ and the $N = 1 \times 10^{17}\,H/cm^2$ implanted areas are clearly damaged, as indicated by the line broadening. For $CuInSe_2$, this behavior was discussed in Refs. [14,15]. The radiation damage, produced by 10 keV hydrogen ions was studied in [2], using Raman as well as RBS-channeling techniques. For an $N = 3 \times 10^{16}\,H/cm^2$ implantation, the defect density in the In sublattice was found to be between 15% and 20% of the In atom density and, therefore, only about 25% of the TRIM prediction. As expected, the spectrum of our $N = 1 \times 10^{17}\,H/cm^2$ implanted area indicates a higher damage level than the spectrum of the $N = 3 \times 10^{16}\,H/cm^2$ implanted $CuInSe_2$ in Ref. [2]. It can be concluded that the $N = 1 \times 10^{17}\,H/cm^2$ implanted area of our sample is heavily damaged with an averaged defect density of more than $1 \times 10^{22}\,cm^{-3}$ in the maximum of the defect depth distribution. "Averaged defect density" means that this estimation neglects effects such as defect clustering. In the Raman spectrum, the $N = 1 \times 10^{15}\,H/cm^2$ implanted area shows no damage. The half-width of the A1 mode at $175\,cm^{-1}$ (which corresponds to the twisting mode of Se atoms [14]) is even slightly reduced with respect to the virgin reference. A similar

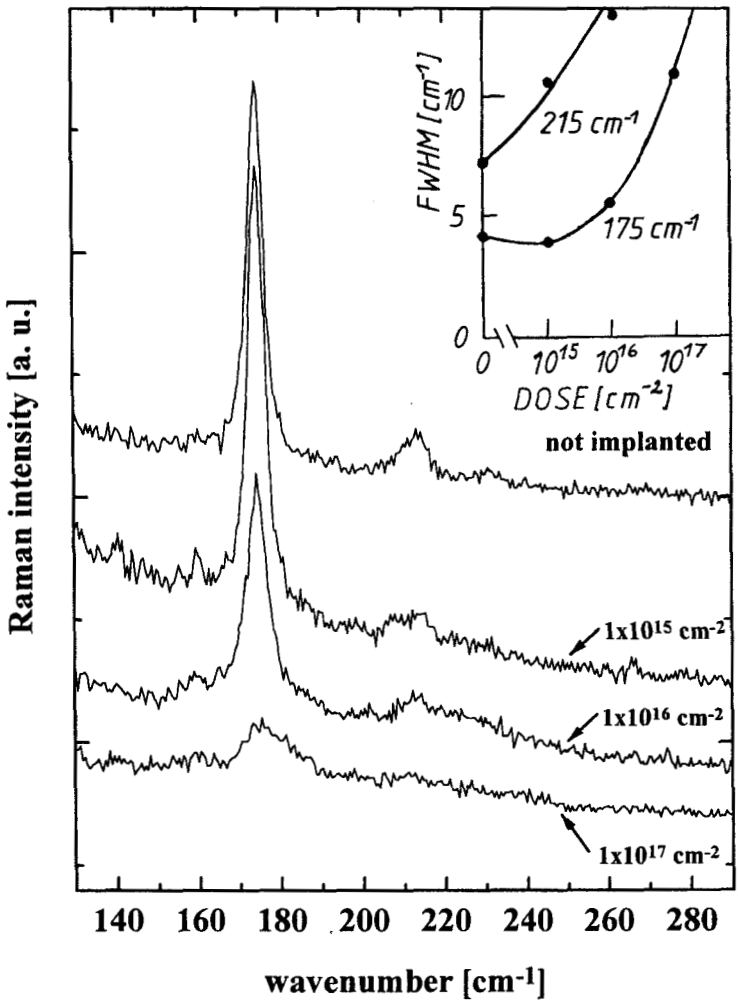

FIGURE 1 Micro-Raman spectra of a $CuInSe_2$ surface before and after hydrogen implantation. Unpolarized detection in backscattering geometry. The insert gives the dose dependence of the full width at half maxima of the two Raman lines.

finding was already reported in [2]. It was explained by a hydrogen passivation of defects.

This effect, and more pronounced, was also found by RBS-channeling [1,2]. RBS also indicated that deeper, not directly implanted layers showed an up to 30% reduction in the defect population due to

hydrogen diffusion. The finding of a defect passivation at low doses and of a lattice damage at high dose levels can only be explained by a nonlinear dependence of the defect production on the dose. Improvement of lattice quality at low doses can only occur if significantly less than one defect is produced per implanted ion. Therefore, the $N = 1 \times 10^{15}$ H/cm^2 implanted area of our sample can be expected to contain a low concentration of radiation induced defects which are virtually completely passivated by trapped hydrogen. The remaining hydrogen can be considered to be as free to distribute within the volume as it would be in a virgin $CuInSe_2$ crystal. For the $N = 1 \times 10^{16}$ H/cm^2 implanted area, Raman already shows an increased defect density. The spectrum is very similar to that shown in Ref. [2], where hydrogen was implanted into $CuInSe_2$ with 10 keV up to a dose of $N = 1 \times 10^{16}$ H/cm^2. At this dose level, there are clearly two depth ranges. The surface-near layer shows implantation induced damage in the Raman spectrum. Because of the high absorption coefficient, again increasing during amorphisation, the Raman information depth is about 50 nm which is only a part of the damage depth profile. RBS-channeling, however, still detects a depth range with decreased defect density deeper inside the sample, before at even higher doses the damage in the upper layer prevents RBS analysis due to screening effects [2]. Therefore, a complex defect distribution can be expected in our $N = 1 \times 10^{16}$ H/cm^2 implanted sample.

Around the maximum of the defect distribution, there is a concentration of implantation induced defects, which can be estimated from an extrapolation of the data given in [2] to be about a few percent of the lattice atom concentration. Between the surface and the maximum of the defect distribution, the defect concentration is similar to the hydrogen concentration. Therefore, in this depth range a significant part of the hydrogen could be trapped due to hydrogen–defect bonds. Below this layer, however, the hydrogen concentration exceeds the defect concentration. After passivation of possible hydrogen traps, the remaining hydrogen could be as mobile as found in the $N = 1 \times 10^{15}$ H/cm^2 implanted area. A variation of hydrogen mobility and, therefore, of the diffusion coefficient with the depth can be expected.

This is in fact found. Figure 2 compiles all depth profiles measured after the implantation at room temperature (solid circles), and after subsequent annealing at 473 K, 30 min (squares). Besides the absolute

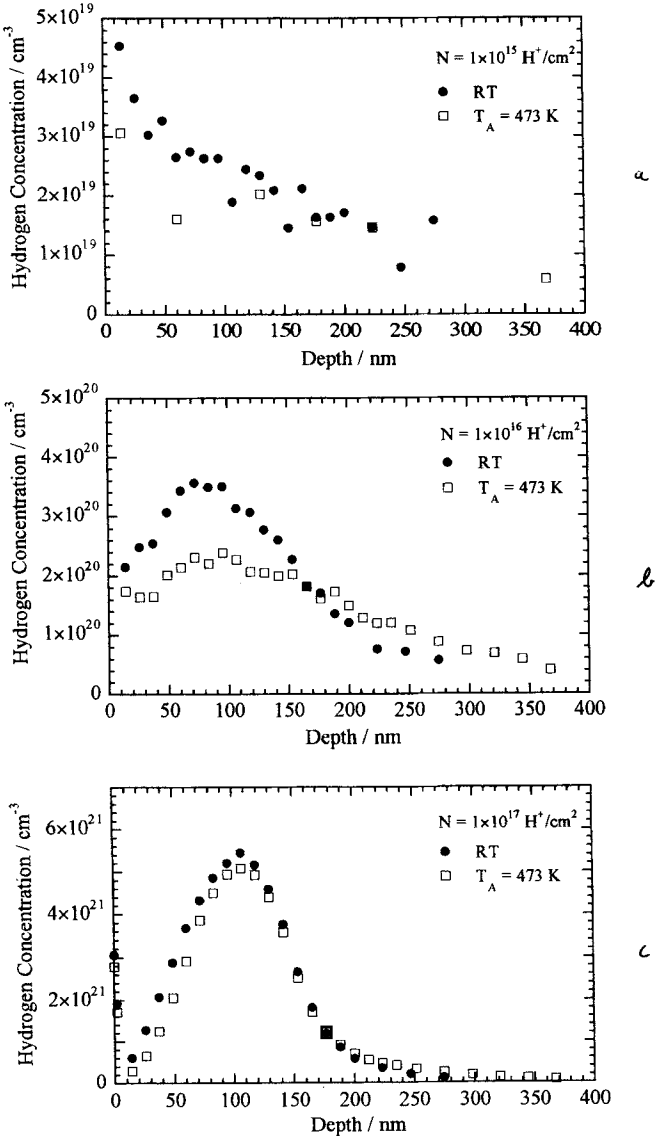

FIGURE 2 Depth distributions of 20 keV H_2^+ implanted into $CuInSe_2$ layers, as-implanted at room temperature (full circles), and after thermal annealing at $T_A = 473$ K for 30 min (open squares). Shown for three different doses, (a) $N = 1 \times 10^{15}$, (b) $N = 1 \times 10^{16}$, and (c) $N = 1 \times 10^{17}$ H/cm^2. The hydrogen surface concentration in cases (a) and (b) is so large (around 6×10^{20} H/cm^{-3}) that it could not be included in the figure.

values of the concentrations, which scale approximately with the dose, also the shapes of the depth distributions are different for the three cases. As will be shown later, none of the distributions coincides with the ballistic distributions as calculated by TRIM [13]; thus some diffusion occurred during implantation and/or in the three weeks storage time at room temperature before the measurement. Qualitatively, the different shapes of the distributions must be the result of diffusities which depend on the dose.

A quite clear change of the depth distributions can be seen for the $N = 10^{16}$ H/cm^2 case after annealing. The peak concentration is reduced, and the concentration in the deeper sample region is increased, indicating a diffusional broadening of the distribution. In the lower profile ($N = 10^{17}$ H/cm^2) the difference between the distributions before and after annealing is found mainly at the surface-near slope of the distribution, indicating an outdiffusion from this region. The concentration in the maximum and deeper inside remains essentially constant indicating a low hydrogen mobility in this region due to trapping. In the low dose case ($N = 10^{15}$ H/cm^2) the poor statistics prevents a meaningful discussion of the redistribution of hydrogen by annealing.

In Figs. 3(a)–(d) the experimental data are replotted and compared with the results of the diffusion simulation described above. The diffusion simulation at $Dt = 0$ in Fig. 3(a)–(d) corresponds to the predicted initial ballistic distribution (TRIM [13]) which in no case agrees with the measured data. In order to find out the reason of the driving force for the observed deviation, we tried several ways with the following possible and physically reasonable assumptions:

(a) The material is not defect-free, i.e. it contains a homogeneous background of deep saturable or unsaturable traps: *The simulations show that this assumption alone does not lead to the measured distributions.*

(b) The material is free of deep traps, but contains shallow traps, especially in the surface-near region. A homogeneous background of shallow intrinsic traps with $A \approx B$ cannot be excluded. These traps lead to a somewhat lowered ('hindered') hydrogen mobility. *The simulations show that this assumption leads to a good description of the observed profile, without any further additional assumptions.* Therefore, we conclude that the hydrogen diffusion in ion

implant-damaged $CuInSe_2$ is governed by shallow traps which have their maximum density in the surface-near region, as described by this second case.

Due to the multitude of mathematically possible variabilities in the input distributions of this program, one might be afraid that this approach is not capable to give a unique answer to the question of the diffusional mechanisms. Our experience shows, however, that in general only one physically reasonable input condition exists which leads to the measured distributions – this is given here also –, and that all other attempts fail by far to fit the observed data. If this happens not to be the case, and several fit possibilities show up (as is given, e.g. in the cases of Li implantation into PP [8], or of LiCl solution penetration into an ion-irradiated PEEK [9]), a decision about the proper modelling can readily be drawn by an additional suitable control measurement. In view of the appreciable sensitivity of the simulated depth profiles to the input values we regard the solution found by us as the only one which describes the given system properly.

In order to find out the detailed depth distribution of these shallow traps, we have applied a trial-and-error technique, by modifying the trap input distribution, and comparing the simulated hydrogen profile with the measured one. Figures 3(a)–(d) show the best fit results, and Fig. 4 illustrates the depth distributions of the product of the hydrogen diffusion coefficients $D(x)$ and time t, which are required to obtain these results. These Dt values (left scale) are taken to describe the sum of both possible thermal and/or radiation enhanced diffusion processes which may take place during and after the implantation until the time of measurement (in our case 3 weeks storage time at ambient temperature). For the case that radiation enhanced mobility does not occur or is negligible, the right scale of Fig. 4 presents the corresponding thermal diffusion coefficients. Hydrogen, being a gaseous dopant, is capable to leave the material when arriving at the sample surface. We have included this boundary condition in our calculation.

As we pointed out already above, the meaning of the derived diffusion coefficient may be that of an effective one, so that the hydrogen mobility in (not yet available) perfectly defect-free $CuInSe_2$ will be higher than the one derived here. In fact, Bridgman-grown $CuInSe_2$ is known to be a defect-rich material with some 10^{19} defects cm^{-3}, their

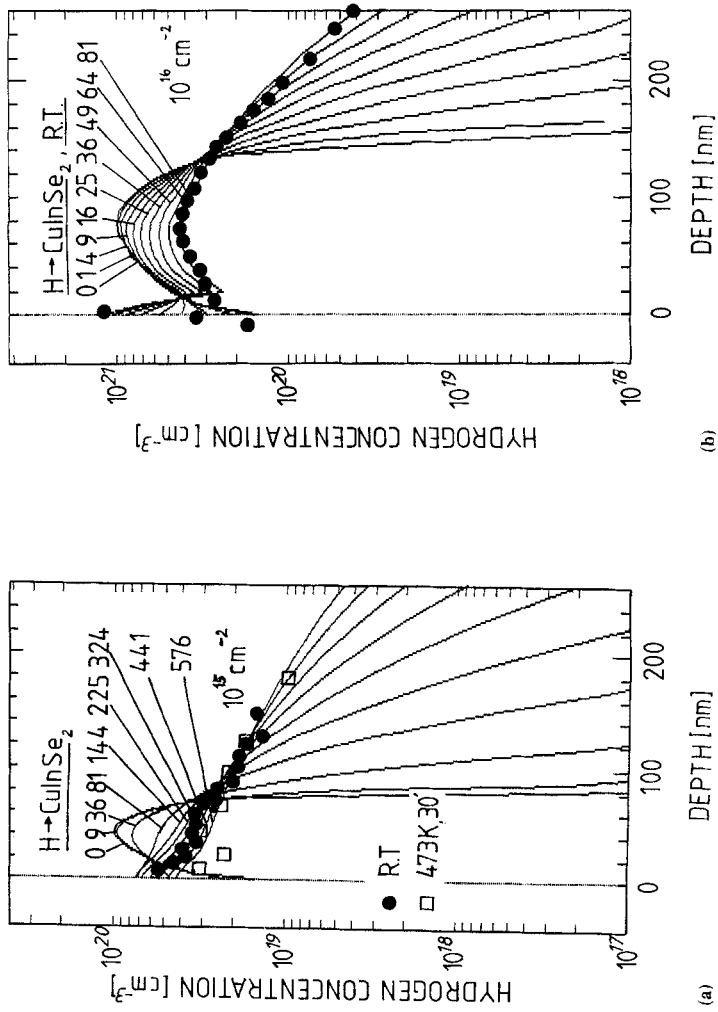

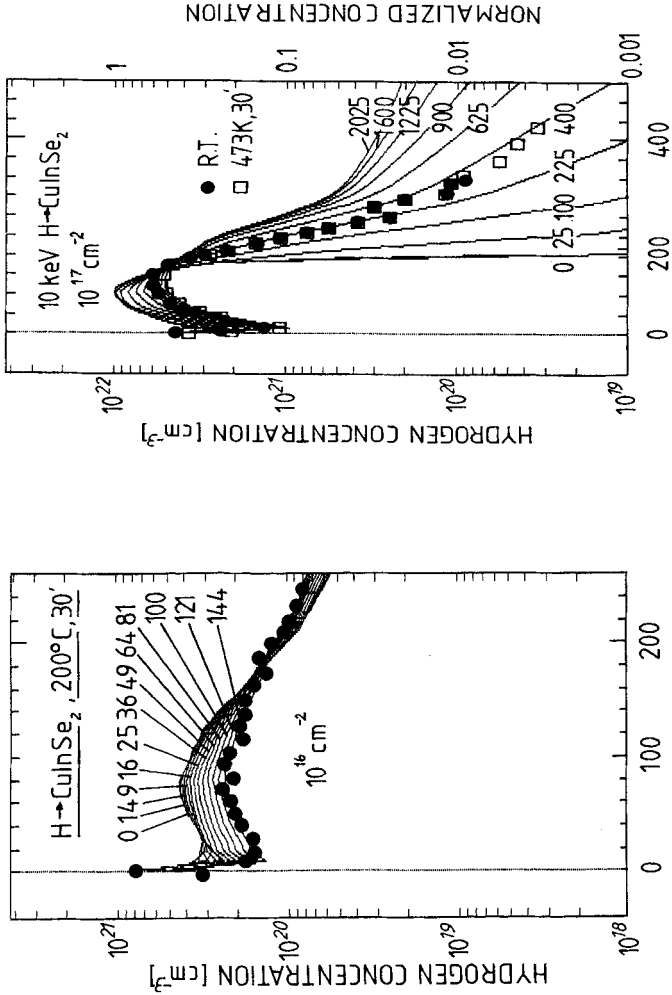

FIGURE 3 Simulation of the 10 keV (H_2^+) hydrogen implantation into $CuInSe_2$ at different H doses, (a) $N = 1 \times 10^{15}$, (b) and (c) 1×10^{16}, and (d) 1×10^{17} H/cm^2. As initial distribution (curve 0) in simulations (a), (b), and (d), the theoretical prediction of the range profile according to Biersack's ballistic Monte Carlo simulation code 'TRIM' [13] (in its commercial 1991 version) is taken. The subsequent curves are simulations of the diffusional redistribution of hydrogen. The numbers denote the simulation cycles, each cycle corresponding to $Dt = 3.3 \times 10^{-13}$ cm^2. The filled circles correspond to the RT measurements, the open rectangles in (a) and (d) denote the depth distributions after thermal annealing at 473 K for 30 min. For the $N = 10^{16}$ H/cm^2 case the room temperature distribution and the distribution after annealing are shown separately (b and c).

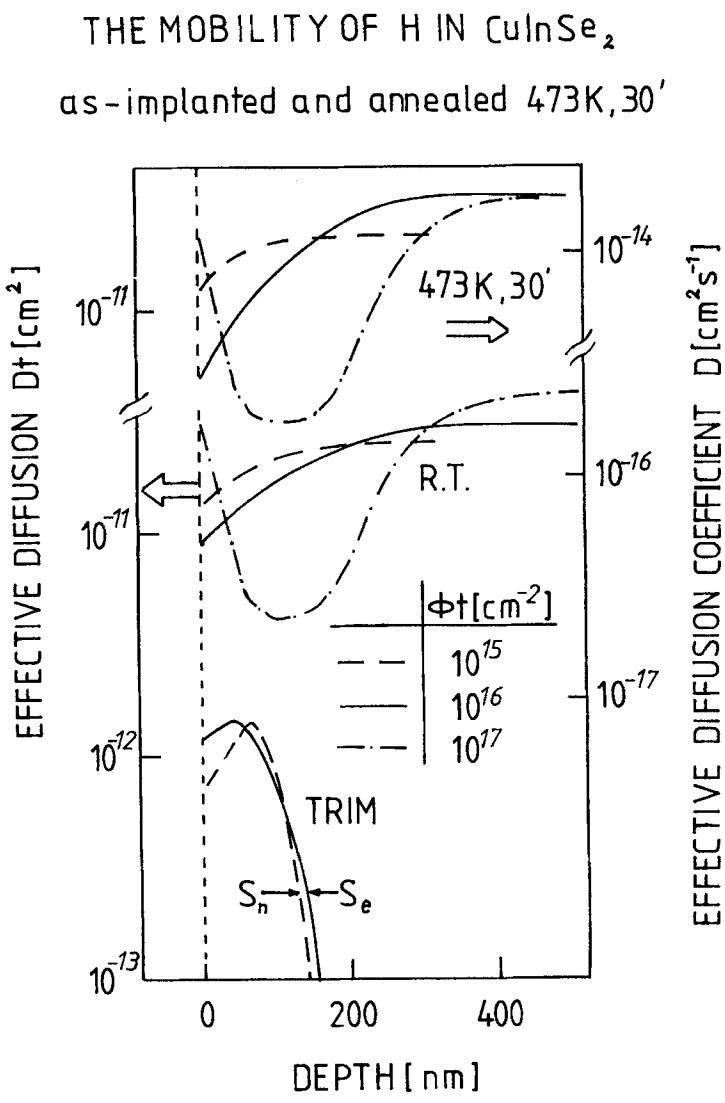

FIGURE 4 Best-fit results of the product of the depth dependent diffusion coefficients and time, $D(x)t$ (left scale), as obtained from the diffusional simulations at RT and 473 K. In the latter case the diffusion coefficient $D(x)$ can be calculated from the Dt values, right scale. The surface-near parts of all curves show strong variations with implanted ion dose. A comparison with the distributions of the nuclear and electronic energy transfer after the hydrogen irradiation shows that there does not exist any directly obvious correlation between the diffusion coefficients and damage distributions.

exact concentration depending on the degree of deviation from stoichiometry. This points at the presence of a background of shallow homogeneous traps, hence at a hindered hydrogen diffusion. On the other hand, there exist speculations that intrinsic defects in $CuInSe_2$ might cluster to rather inert defect complexes which hardly are capable to trap hydrogen. Therefore we have to leave the answer still open, in how far the measured bulk hydrogen diffusion coefficient depends on the material's intrinsic defects, until $CuInSe_2$ crystals of better quality will be available for comparison.

The fact that the effective hydrogen mobility in the implanted sample is lowered strongly in the sample's surface-near area, in comparison with its bulk value, indicates that here radiation defects add to the intrinsic ones. Let us consider the few values which are available at present:

- unimplanted (reference material for D_{eff}): 10^{19} defects/cm^3,
- 1×10^{16} cm^{-2} implanted: lowering of D_{eff} by a factor of 3 to 5,
- 3×10^{16} cm^{-2} implanted: about 5×10^{22} defects/cm^3 [2],
- 1×10^{17} cm^{-2} implanted: lowering of D_{eff} by about a factor of 10, and more than 10^{22} defects/cm^3 [2].

It appears that the lowering of D_{eff} is roughly proportional to the overall defect density. This may indicate that the nature of both the intrinsic and the irradiation-induced defects is similar to each other.

For low dose implantation ($N = 1 \times 10^{15}$ and 1×10^{16} H/cm^2), the trial-and-error results point at simple exponential correlations between $D(x)$ and x in the surface-near region: $D(x) = D_0 \cdot (1 - \exp(-c \cdot x))$, with different slopes c. A reduction of the diffusion coefficient in relation to the bulk value signifies that there exist shallow traps which lead to this hindered trapping–detrapping mobility. Obviously, both the trap density and the width of the trap-enriched zone increase with dose. The comparison with the distributions of the ion-induced damage (also included in Fig. 4) reveals that there does not exist any simple correlation between the fitted distribution $D(x)$ and the collisional or electronic energy transfer from the hydrogen ions. But keep in mind that the statistical accuracy of the H depth profile measurement at the lowest dose – and hence the reliability of the reconstructed diffusion coefficient distribution – is somewhat poor, in contrast to the higher implanted doses.

The simulation of the high dose case ($N = 1 \times 10^{17}$ H/cm^2) leads to an even broader and deeper-lying zone of strongly reduced hydrogen mobility. In striking contrast to the low dose case however, it is seen that the mobility is quite high in the direct surface-near zone. Again, no simple correlation between the fitted distribution $D(x)$ and the collisional or electronic energy transfer from the hydrogen ions shows up.

The surface-near depletion of the derived effective diffusion coefficients by up to an order of magnitude signifies that the A/B ratio ranges up to 10, i.e. that the strength of the surface-near traps approaches to the one of deep traps in these extreme cases.

In all cases the deviations from the bulk value D_0 extend some 2–3 times deeper into the bulk than the predicted ballistic damage distributions. The possibility to explain these puzzling findings by assuming that the primary radiation induced collisional defects – interstitials and/or vacancies, which act as traps – are mobile in $CuInSe_2$ at room temperature and under implantation conditions fails, as defect profiles measured recently by HRTEM [16] and REM [17] always have shown good consistency with the ballistic predictions [13], as far as concerns the shape of their depth distribution. Discrepancies occurred only in the absolute defect concentrations, as the ballistic code TRIM does not include defect annealing processes. Hence the damage distributions can be considered as being immobile. Therefore we suggest the following model:

Hydrogen implantation into p conducting $CuInSe_2$ leads to the formation of an n conducting surface layer, hence to a p–n homojunction [4], as the implanted hydrogen concentration practically always exceeds the hole concentration (around 10^{16} cm^{-3} for virgin samples [4]). For example, recent EBIC measurements of such a 10 keV, $N = 5 \times 10^{16}$ H/cm^2 hydrogen implanted $CuInSe_2$ layer have shown that the depletion layer just begins at a depth of 350–400 nm, extending down to some 2 μm (unpublished work). Taking into account that hydrogen in semiconductors usually exists as a charged ion (H^- in n conducting, and H^+ in p conducting material), one hence may speculate that different diffusitivities exist in the n- and p-type regions, respectively. But other explanations, e.g. concentration dependent H_2 formation, etc., are also possible.

There exists frequently a strong surface peak in the measured hydrogen profiles. On the one hand, this stems from the hydrogen

content of the surface hydrocarbon contaminant layer. It also might indicate that not all surface hydrogen is capable to leave the sample, but that some is bound permanently at this thin layer. We have simulated the influence of such a layer by assuming that the surface contains unsaturable traps. The simulation shows that this surface layer cannot be thicker than at maximum 10–15 nm in the case of the $N = 10^{16}$ H/cm^2 implantation, and some 5 nm only in the $N = 10^{17}$ H/cm^2 case. The surface layer acts as a diffusion barrier with limited efficiency, with the Dt value for hydrogen ranging from 10^{-10} to 10^{-9} cm^2, and the trapping efficiency A ranging from 0 to 0.1.

In the same way as we have simulated the as-implanted profiles, we could also simulate the subsequent thermal annealing process, see Figs. 3(a),(c) and (d), and Table I. Figure 4 shows that the thermal annealing process hardly changes the shape of the depth distribution of hydrogen mobility, but essentially changes the absolute values of mobility. This signifies that, though the thermal annealing of H implanted $CuInSe_2$ enhances the hydrogen mobility, it does not yet lead to a major change in the defect spectrum, e.g. by formation of small mobile defects at the expense of large immobile ones. The only hint for such an effect is that the concentration of the shallow traps in the intermediate dose (10^{16} cm^{-2}) case at elevated temperature is roughly twice as high as in the room temperature case.

The computer simulations show that *all measured surface-near H distributions consist of both free and trapped components.* It will be of great interest to repeat the room temperature measurement of the depth distributions sometime later, in order to get more information about the detrapping probability from the shallow surface-near traps. In fact, similar experiments on the long-time stability (within typically some 5

TABLE I Dt-values (product of the diffusion coefficient D and time t) at room temperature and after annealing at 473 K, 30 min. Second column: for the bulk average of all three samples and for the region of the lowest diffusitivity (50–150 μm depth). The values in the third column are given for the dose $N = 10^{17}$ H/cm^2 only

T[K]	Dt [cm^2] (bulk)	Dt [cm^2] (maximum)
293	$(1.9 \pm 0.8) \times 10^{-11}$	4.1×10^{-11}
473 30′	$(2.5 \pm 0.8) \times 10^{-11}$	3.2×10^{-11}

years) of boron in metals [18] have shown that the implantation distributions are metastable in many systems.

5. CONCLUSIONS

Hydrogen ions have been implanted into the semiconductor material $CuInSe_2$ at different doses. As the ions act as a probe for the self-created material's damage, it is possible to derive information about the distribution of traps from the hydrogen distribution. In the same way, recently the damage of polypropylene foils by Li ions was determined from the depth distribution of self-trapped Li ions [8]. In our specific case it turns out that

(a) hydrogen does not come to rest immediately after the ballistic implantation, but still keeps some limited mobility;
(b) there exists no background of deep traps in the bulk material, but that shallow traps are present, consistent with the material's high defect density;
(c) there exist additionally shallow traps with partly considerable bonding strengths in the surface-near implanted region and slightly beyond which lead to a reduction of the hydrogen mobility;
(d) the trap concentration and distribution depends on the damage introduced by the hydrogen ions;
(e) the shape of the trap distribution does not follow the shape of either electronic or nuclear proton damage depth distributions;
(f) a hydrocarbon surface layer of 5–15 nm – such as created under poor vacuum conditions during implantation – is capable of trapping hydrogen permanently; and
(g) thermal heating up to 473 K enhances the hydrogen mobility but leaves the trap distribution unchanged.

Acknowledgements

We want to thank the crew of the Ion Beam Lab (ISL) of the HMI for their help in enabling this work. One of the authors (KKD) acknowledges financial support by the DAAD, one (SG) support by the Indian government, and another one (WHC) by the KOSEF and the DFG.

References

[1] M.V. Yakushev, R.D. Tomlinson and H. Neumann, *Cryst. Res. Technol.* **29** (1994) 125.
[2] M.V. Yakushev, G. Lippold, A.E. Hill, R.D. Pilkington and R.D. Tomlinson, *Cryst. Res. Technol.* **31** (1996) 357.
[3] M.V. Yakushev, R.W. Martin, G. Lippold, H.W. Schock, J.A. Van den Berg, D.G. Armour, R.D. Pilkington, A.E. Hill and R.D. Tomlinson, *Book of Abstracts, 14th European Photovoltaic Solar Energy Conference*, 30 June–4 July 1997, Barcelona, Spain.
[4] M.V. Yakushev, H. Neumann, R.D. Tomlinson, P. Rimmer and G. Lippold, *Cryst. Res. Technol.* **29** (1994) 417.
[5] M.V. Yakushev, A. Zegadi, H. Neumann, P.A. Jones, A.E. Hill, R.D. Pilkington, M.A. Slifkin and R.D. Tomlinson, *Cryst. Res. Technol.* **29** (1994) 427.
[6] L.T. Chadderton, *Rad. Effects* **8** (1971) 77.
[7] D. Fink, J. Krauser, D. Nagengast, T. Almeida Murphy, J. Erxmeier, D. Bräuning, A. Weidinger and L. Palmetshofer, *Appl. Phys. A* **61** (1995) 381.
[8] D. Fink, M. Behar, J. Kaschny, R. Klett, L.T. Chadderton, V. Hnatowicz, J. Vacik and L. Wang, *Appl. Phys. A* **62** (1996) 359–367.
[9] D. Fink, J. Vacik, Y. Kobayashi, R. Klett, V. Hnatowicz, *Nucl. Instr. Meth.* **B134** (1998) 61–72.
[10] M.V. Yakushev, G. Lippold, A.E. Hill, R.D. Pilkington and R.D. Tomlinson, *J. Material Science: Materials in Electronics* **7** (1996) 155.
[11] W.A. Lanford, H.P. Trautvetter, J.F. Ziegler and J. Keller, *Nucl. Instr. and Meth.* **149**(1) (1976) 566.
[12] J. Krauser, F. Wulf and D. Bräunig, *J. of Non-Crystalline Solids* **187**, (1995) 264.
[13] J.P. Biersack and L.G. Haggmark, *Nucl. Instr. Meth.* **174** (1980) 257.
[14] M. Nishitani, T. Negami, S. Kohiki, M. Terauchi, T. Wada, T. Hirao, *J. Appl. Phys.* **74** (1993) 2067.
[15] G. Lippold, M.V. Yakushev, R.D. Tomlinson, A.E. Hill and W. Grill, *Cryst. Res. Technol.* **31** (1996) 381.
[16] C.A. Mullan *et al.*, *Phil. Mag. A* **73** (1996) 1131.
[17] M.V. Yakushev *et al.*, *Cryst. Res. Technol.* **31** (1996) 357.
[18] D. Fink and L. Wang, *Rad. Eff. Def. Sol.* **114** (1990) 343–371.